Continuous wide-field characterization of drug release from skin substitute using off-axis interferometry

Haniel Gabai, Maya Baranes-Zeevi, Meital Zilberman, and Natan T. Shaked*

Department of Biomedical Engineering, Faculty of Engineering, Tel-Aviv University, Tel-Aviv 69978, Israel
Corresponding author: nshaked@tau.ac.il

We achieved continuous, noncontact wide-field imaging and characterization of drug release from a polymeric device *in vitro* by uniquely using off-axis interferometric imaging. Unlike the current gold-standard methods in this field, which are usually based on chromatography and spectroscopy, our method requires no user intervention during the experiment and involves less lab consumable instruments. Using a simplified interferometric imaging system, we experimentally demonstrate the characterization of anesthetic drug release (Bupivacaine) from a soy-based protein matrix, which is used as a skin substitute for wound dressing. Our results demonstrate the potential of interferometric imaging as an inexpensive and easy-to-use alternative for characterization of drug release *in vitro*.   © 2013 Optical Society of America

Release rate and duration are the principal characteristics of drug release from a polymeric drug delivery device (DDD), and monitoring them is highly important for evaluating the desirable local therapeutic effects. The prediction of these desirable characteristics when designing a DDD is a challenging task, since the *in vivo* drug release mechanisms are influenced by a variety of factors such as drug and DDD composition, DDD shape, drug location within the DDD, type and pH of the immersion medium, and many other factors [1,2]. Due to this complexity, a comprehensive set of drug release monitoring experiments are needed in order to evaluate the drug release properties of the DDD. Existing methods for this task include x-ray computed tomography (CT) [3], positron emission tomography (PET) [4], and magnetic resonance imaging (MRI) [5]. However, the latter two techniques use ionizing radiation, and all three are highly expensive and require well-trained operators, making them less attractive for clinical use.

An alternative approach for evaluating the drug release properties of the DDD *in vivo* is to perform a comprehensive set of *in vitro* drug release monitoring experiments. Next, extrapolation from the *in vitro* experiments into an *in vivo* model is needed. Better understanding of the *in vitro* drug release process can significantly improve the extrapolation to the *in vivo* device and may reduce the use of *in vivo* experiments.

These *in vitro* measurements are currently performed by the analysis of indirect concentration measurements from the DDD immersion medium. The gold-standard modalities for performing this task include spectroscopy and high-performance liquid chromatography (HPLC). HPLC is based on the separation of the components in a mixture by its pressurization via pumps into a column filled with sorbet. The components are then detected by a spectrophotometer. Next, a fitting process between the results obtained by HPLC to the several known concentration measurements is performed [6].

However, HPLC is highly expensive and suffers from several limitations. For instance, during the experiment, an extraction of the DDD immersion medium is required, a process that is considered intrusive. Moreover, to achieve the release profile over time, a test tube is filled with an immersion medium for each measurement. For example, for 24 h analysis of a single DDD, where a test tube is taken every hour, 24 test tubes are taken and analyzed by the clinician. To perform longer experiments with better time resolution, analysis of tens of test tubes is needed. This makes these experiments highly expensive in terms of man hours and lab consumable instruments. Moreover, the large amount of test tubes used and the routine labor increase the chance for human errors. Therefore, time resolution in HPLC measurements is typically poor.

Another disadvantage of the existing gold-standard modalities is that they provide one measurement per time rather than image many spatial points. Such information might have a clinical value when trying to characterize the spatial distribution of drug within the test tube, especially from inhomogeneous DDDs or in evaluating the diffusion time of drug from the DDD to the target through different media.

In this Letter, we suggest using wide-field off-axis interferometry as an alternative modality for characterization of drug release from DDDs *in vitro*.

Our underlying assumption is that drug release will result in an immediate local change in the refraction index of the immersion medium and, consequently, a local change in the spatial quantitative phase profile, which can then be continuously measured by interferometry. In contrast with the traditional modalities, when using interferometry only a single test tube has to be prepared, no intervention is needed during the experiment, the spatial drug distribution within the immersion medium can be imaged, and significantly higher time resolution can be achieved, limited only by the full frame rate of the camera. This is especially useful when characterizing
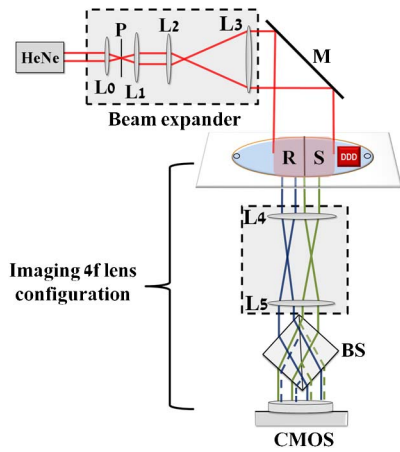
Fig. 1.   Experimental setup. HeNe: Helium–Neon laser; L0-5: lenses (f = 35, 50, 45, 150, 75, 40 mm); P: 25 μm pinhole; M: mirror. The coverslip is covered by a chamber-like silicon sticker, divided by a thin silicon bar into two sections coinciding with the reference arm R and sample arm S. DDD: drug delivery device (located outside the FOV); BS: beam splitter; blue lines: reference arm; green lines: sample arm; solid lines in the BS: transmitted light; dashed lines in the BS: reflected light; CMOS: conventional CMOS camera (DCC1545M, Thorlabs, 1280 × 1024 square pixels of 5.2 μm²).

the first hours of a drug release process, when the drug concentration increases rapidly, or for certain rapidly eluting DDDs during the entire drug release process.

For this purpose, we have modified the wide-field, off-axis interferometric imaging system presented by us in Ref. [7]. As shown in Fig. 1, this simplified, low-cost, interferometric imaging system is illuminated by an expanded He–Ne laser beam and is based on a single beam-splitter cube positioned at the output of the system. This beam splitter serves as a common-path interferometer, where half of the beam serves as the interferometric reference beam, and the second half serves as the interferometric sample beam [7,8]. Both beams are projected onto the camera using a 4f lens configuration, where the sample interferogram is recorded. This simplified, close-to-common-path design significantly reduces the need for additional optical elements required for Linnik's or other conventional and harder-to-align interferometric imaging configurations. Hence, no special optical expertise is needed for the construction and operation of the proposed system, making it ideal for clinical and low-resource industrial use.

Drug release from a DDD is a dynamic process, as the drug leaves the DDD and spreads within the surrounding medium. The presence of the drug within the medium results in a local change in its refractive index, and thus it can serve as a drug concentration indicator at a given location and time. Then, in similarity to the HPLC procedure, a calibration of the acquired measurements to given cumulative drug concentration (i.e., percentage of drug left the DDD) measurements is performed.

The DDD used in our experiments is a soy-based protein matrix [9,10], which is utilized as a skin substitute for treating wounds, especially severe and large burns.

This unique DDD is inexpensive, easily generated, biocompatible, has a nonanimal origin (i.e., there is no risk

for transferring diseases), and eventually degrades into natural components. In our experiment, the DDD contained 3% of Bupivacaine anesthetic drug (0.34 mg).

To prepare the sample for imaging, a 5 mm × 3 mm DDD was placed on a coverslip covered by a chamber-like silicon sticker (32 mm × 17 mm CoverWell perfusion chamber). As demonstrated in Fig. 1, the DDD was positioned at the periphery of the silicone chamber, outside the imaging field of view (FOV) in order to avoid diffraction and multiple scatterings artifacts while ensuring the drug will diffuse into the FOV. The drug release was monitored over time by capturing only the area containing the immersion medium plus drug within the sample chamber, where the imaging system ensured that almost the entire area was imaged at once.

Since in the proposed system the other side of the chamber contains the medium only, and thus serves as the interferometric reference section, there is a need to ensure that no drug will diffuse into this section. This is performed by dividing the total volume of the chamber into two sections by a thin silicon bar (see Fig. 1).

Prior to imaging, each section of the chamber was slowly filled with 150 μl of phosphate-buffered saline (PBS) using the perfusion ports, which gradually started the drug eluting process due to diffusion. No enzymes were introduced to the PBS in order to avoid DDD degradation. Then the perfusion ports were immediately sealed by stickers, preventing leakage of the medium outside the chamber and the wave-like motion of fluid inside.

The quantitative phase profile of the sample is numerically reconstructed from the recorded off-axis interferogram using a digital two-dimensional Fourier transform, followed by spatial filtering of the sample field and an inverse Fourier transform. Next a phase unwrapping digital process is performed on the argument of the result [7,11].

Phase profile is defined as $\varphi(x, y) = 2\pi/\lambda \times \text{OPD}(x, y)$, where λ is the illumination wavelength, and

$$
\begin{aligned}
\text{OPD}(x, y) &= \int_0^{h_{\text{tot}}} [n_{\text{tot}}(x, y, z) - n_m]\mathrm{d}z \\
&= h_d(x, y)n_d + [h_{\text{tot}} - h_d(x, y)]n_m - h_{\text{tot}}n_m \\
&= h_d(x, y)[n_d - n_m]
\end{aligned}
\tag{1}
$$

is the optical-path-delay profile, where n_{tot} is the refractive index within the sample section, n_m is the medium constant refraction index (e.g. within the reference section), h_d is the overall thickness of the drug at each point, n_d is the refraction index of the drug, and h_{tot} is the total medium thickness within the immersion chamber. When examining Eq. (1), it can be seen that when imaging in a close chamber with a fixed thickness, the quantitative phase in each lateral position is proportional to the drug thickness and thus to the quantity of the drug eluted to the medium. Hence, it serves as an equivalent value to the cumulative drug concentration, which is an important parameter for characterizing drug release [1,2].

Note that since the reference beam passes through the chamber with PBS only, in time zero we get zero drug
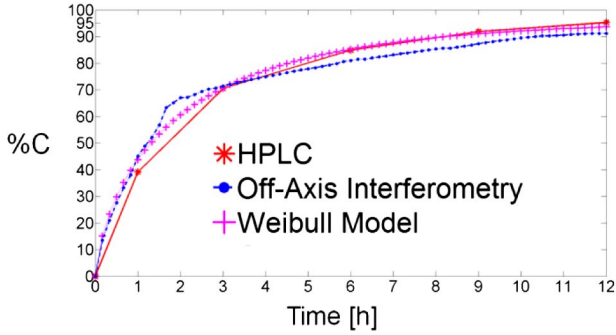
Fig. 2.   Cumulative drug-release profiles obtained from HPLC (solid line), off-axis interferometry (dotted line), and Weibull model (crossed line) for drug release period of 12 h.

concentration. Thus, this self-referencing system is unbiased according to the zero concentration point.

The solid red line in Fig. 2 presents the five drug-release measurements taken by HPLC (Jasco, UV 2075) [10]. As can be seen from this graph, the release is characterized by relatively fast drug release of more than 85% of the total drug amount within the DDD in the first 6 h. Then, for the following 6 h, a moderate release of an additional 10% occurs. The remaining 5%, which has less clinical importance, is slowly released during 13 additional days.

To test our hypothesis, the DDD was continuously monitored using the proposed interferometric system for 12 h with a sampling rate of one frame per 10 min, resulting in 73 measurements. Achieving such time resolution with HPLC is highly difficult and expensive.

Figure 3 and Media 1 present the spatial phase profile of the entire FOV, as obtained by the off-axis interferometric system followed by the digital process described above. As seen from this figure, significant temporal and spatial changes are observed in the quantitative phase profile within the FOV due to drug release from the DDD. In areas that are in close proximity to the DDD, the most significant changes in the phase values are observed, whereas in areas distant from the DDD, the phase changes are more moderate.
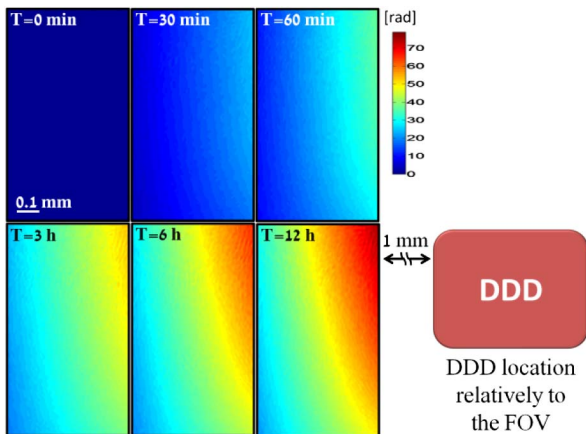

Fig. 3.   Quantitative phase profile resulted from drug release during 12 h, as measured by continuous wide-field interferometric imaging. The right lower frame illustrates the DDD location relatively to the FOV. See full dynamics in Media 1.

For each frame captured, the averaged phase value of the entire spatial phase distribution was calculated. The averaged value serves as an indicator on the cumulative drug concentration within the FOV, since the FOV approximately coincides with the entire sample half of the chamber. We then fitted the 73 interferometric measurements to the five HPLC measurements, where our underlying assumption is that the behavior of this curve will be similar and proportional to the actual drug-release profile measured by HPLC, due to the accumulative mathematical property of the quantitative phase profile. This process is similar to the fitting process carried out after HPLC using measurements of known concentrations. For our fitting process, we define the calibration factor α as follows:

$$\alpha = \frac{1}{N} \cdot \sum_{i=1}^{N} \frac{C(i)}{\bar{\varphi}(i)}, \qquad (2)$$

where C is a vector containing the cumulative drug concentrations measured by HPLC (or another method) over time with standard sampling rate (in our case, after 1, 3, 6, 9, 12 h), $\bar{\varphi}$ is a vector containing the averaged phase values sampled in times identical to the sampling times of the HPLC measurements, and N is number of points in vectors C or $\bar{\varphi}$ (five in our case).

Next, to fit the two graphs, we multiplied all 73 averaged interferometric phase values by the calibration factor α. The dotted blue line in Fig. 2 presents the resulting high-temporal resolution graph produced by interferometry. Both HPLC and interferometry curves have the same characteristics, i.e., rapid rise at the first 2 h, which corresponds to the drug-release burst effect, followed by a moderate climb. A Pearson correlation value [12] of 0.9958 is found between vectors C and $\alpha \cdot \bar{\varphi}$ with a mean square error (MSE) of 3.905%.

To check the accuracy of the full, high-time-resolution interferometry-based graph, we have used the Weibull mathematical drug-release model. This model was chosen due to its capability of describing drug release from matrix-type DDDs [13,14,15], such as the one used in this work. According to this model, the drug release is described as follows:

$$C(t) = C_{\text{end}} \cdot \left[1 - \exp \left(\frac{t}{td} \right)^{\beta} \right], \qquad (3)$$

where C_{end} is the concentration after 12 h, td is the time when the cumulative concentration equals 63.2%, and β is a shape parameter. The three model parameters were optimized by fitting $C(t)$ to the HPLC graph using an exhaustive-search algorithm, which employed over 23,000 searches. The initial guesses of the parameters C_{end} and td were based on the HPLC measurements. β was optimized from a large interval of values based on previous works [14,15]. Best fitting to HPLC values was obtained for $td = 2.003$ h, $C_{\text{end}} = 96.4\%$, and $\beta = 0.7105$, which result in the crossed pink line graph shown in Fig. 2.

Table 1 presents the Pearson correlation and the MSE values between the different graphs shown in Fig. 2, showing that the high-time-resolution graph obtained

Table 1.   Comparison between the Different Approaches

Comparison	Pearson Correlation	Mean Square Error (%C)
Interferometry versus HPLC	0.9958	3.905
Interferometry versus Weibull model	0.9914	3.5035
HPLC versus Weibull model	0.9986	2.012

by off-axis interferometry has good compatibility to both the HPLC and the Weibull model graphs.

Moreover, although the Weibull model curve was optimized to the HPLC curve only, the burst effect, which occurs during the first 1.5 h of the measurement and has great clinical importance, almost completely overlaps with the equivalent section in the interferometric curve, demonstrating the necessity of measuring rapid drug-release processes by interferometry.

Another advantage of interferometry is its ability to image in wide field the spatial drug distribution, rather than yielding a single-value measurement at a given time, as done by HPLC. Figure 4 shows the normalized phase profile across the diagonal line in the FOV over time. As can be seen from this figure, in locations closer to the DDD, more significant temporal changes are seen. In distant locations, a certain delay in the onset of the drug-release profile is observed, and its amplitude is significantly lower. Both the late onset and low amplitude become more significant when examining distant locations from the DDD. This additional spatial information cannot be provided by HPLC and may have great value for clinicians exploring the spatial effects of drug release and for mathematicians trying to model this process.

The total drug amount detected in our case is 91.2%C (0.31 mg). The mean spatial phase noise within the FOV is 0.0343 rad, and after multiplying it by the calibration factor α, we calculated the concentration sensitivity that can be obtained by interferometry in our case as 0.069%C (0.234 μg). Although HPLC can theoretically provide higher sensitivity of up to 10^{-4}%C, for drug-release applications, where the concentration difference between two adjacent measurements is relatively high, the sensitivity provided by interferometry is sufficient.

In conclusion, we introduced a method for *in vitro* wide-field imaging and characterization of drug release from DDDs with good compatibility to HPLC, which is considered as the gold-standard modality for this task. In contrast with HPLC, our system is inexpensive and requires only single sample preparation for the entire experiment. Moreover, no intervention of a clinician is needed during the experiment, and thus the method is nondestructive, with lower chances for human errors. In addition, the measurement is continuous, and time resolution is determined by the full frame rate of the camera. The significantly higher time resolution obtained by interferometry can be helpful when trying to characterize specific time periods of fast drug release, such as the drug burst effect or when measuring fast-releasing DDDs.
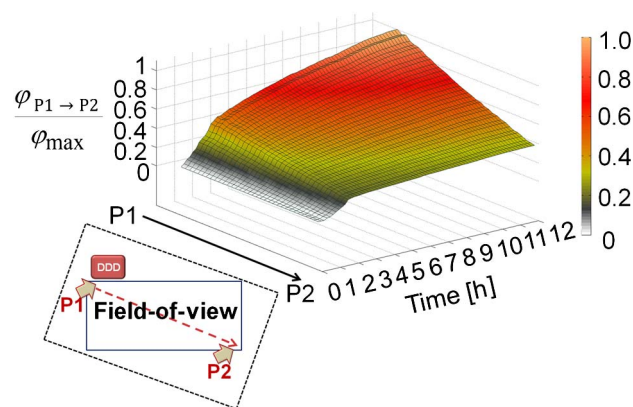

Fig. 4.   Normalized dynamic phase profile, used as local drug-release estimator, for 34 locations, starting from the most proximate location to the DDD (marked as P1) to the most distant location from the DDD (marked as P2).

With good correlation to both HPLC experimental measurements and to a mathematical model, our results demonstrate the high potential of interferometry in wide-field characterization of drug release from DDDs. In addition to drug-release monitoring, a prospective closely related application of off-axis interferometry is for providing direct imaging of DDD degradation, which is a crucial factor in the drug-release mechanism and in tissue-engineering applications.

References

1. J. Heller, Biomaterials **1**, 51 (1980).
2. L. G. Griffith, Acta Mater. **48**, 263 (2000).
3. A. Szymanski-Exner, N. T. Stowe, K. Salem, R. Lazebnik, J. R. Haaga, D. L. Wilson, and J. Gao, J. Pharm. Sci. **92**, 289 (2003).
4. A. Bhatnagar, R. Hustinx, and A. Alavi, Adv. Drug Delivery Rev. **41**, 41 (2000).
5. J. S. Taylor and W. E. Reddick, Adv. Drug Delivery Rev. **41**, 91 (2000).
6. L. R. Snyder, J. J. Kirkland, and J. W. Dolan, *Introduction to Modern Liquid Chromatography* (Wiley, 2011).
7. H. Gabai and N. T. Shaked, Opt. Express **20**, 26906 (2012).
8. J. A. Ferrari and E. M. Frins, Opt. Commun. **279**, 235 (2007).
9. Z. Peles and M. Zilberman, Acta Biomat. **8**, 209 (2012).
10. M. Baranes-Zeevi and M. Zilberman, "Formulation-property effects in soy-protein based structure with drug delivery for wound healing applications," J. Biomed. Mater. Res., submitted for publication.
11. J. Mertz, in *Introduction to Optical Microscopy* (Roberts and Company Publishers, 2010), pp. 13–26.
12. L. Rodgers, J. Nicewander, and W. A. Nicewander, Am. Stat. **42**, 59 (1988).
13. S. Dash, P. N. Murthy, L. Nath, and P. Chowdhury, Acta Poloniae Pharmaceutica **67**, 217 (2010).
14. K. Kosmidis, P. Argyrakis, and P. Macheras, Pharm. Res. **20**, 988 (2003).
15. V. Papadopoulou, K. Kosmidis, M. Vlachou, and P. Macheras, Int. J. Pharm. **309**, 44 (2006).